Physics of the Solid State, 2024, Vol. 66, No. 11

05,07

Formation of domain structure in laser-amorphized regions of PrDyFeCoB microwires

© *E.V. Dvoretskaya*[1], *R.B. Morgunov*[1,2]

[1] Federal Research Center of Problems of Chemical Physics and Medicinal Chemistry RAS, Chernogolovka, Russia
[2] Tambov State Technical University, Tambov, Russia

E-mail: Dvoretskaya95@yandex.ru

Received July 18, 2024
Revised October 8, 2024
Accepted November 9, 2024

Local irradiation of the polycrystalline microwire PrDyFeCoB creates a thin layer of amorphous-crystalline material with a depth of $2-3\,\mu$m on its surface. This soft magnetic material with a coercive force of 10 Oe is divided into domains with magnetization directed in the plane of the surface layer. The motion of the domain wall with increasing magnetic field and the absorption of domains of reverse magnetization is the main mechanism in the surface layer. In locally amorphized regions, the dependence of the domain wall velocity on the magnetic field corresponds to the creep mode of domain walls. In completely amorphous microwires, the domain motion velocity is two orders of magnitude higher and demonstrates a transition from the creep mode to the sliding mode.

Keywords: microstructures, magnetic domain structure, laser amorphization, micromagnets, additive technologies.

DOI: 10.61011/PSS.2024.11.60089.198

1. Introduction

It is known that the irradiation of ferromagnets with short laser pulses is not limited to short-term heating alone, and the change of their properties is not explained by a short-term increase of temperature. The effects associated with the fully optical remagnetization of thin ferromagnetic films are described in the literature [1,2], and data on changes of structure and phase composition under the impact of a heat shock wave and the electromagnetic field of a light wave are discussed. Short-term heating by itself is also not equivalent to annealing of the material and it is essentially an extreme state , leading to the occurrence of new metastable phases. The formation of a crater in ferromagnets based on rare earth metals under the action of laser radiation has been studied previously [3,4]. It was found that phases appear as a result of such irradiation that did not exist in the source material, a significant redistribution of chemical elements takes place in the irradiation zone, as well as a significant change of the coercive force and other magnetic properties.

Although NdFeB alloys are the most common type of permanent magnets, their practical application is limited by their high brittleness, significant changes of magnetization with temperature, and the inability to create the desired magnetization geometry in a sintered magnet. Therefore, the compatibility of these properties is achieved by varying the chemical composition of the sublattices of rare earth and transition metals with a slight loss of magnetization in the related PrDyFeCoB alloy. PrDyFeCoB microwires have unusual micromagnetic properties due to the presence of layers, exchange displacement, and switching of magnetization [5,6] and are used for the creation of micropincers in biology [7].

The amorphization of the surface of microwires is also interesting in addition to micromagnetic applications in Micro-Electro Mechanical Systems (MEMS) technologies and it is important because amorphous alloys of this group are usually very durable coatings which are resistant to external chemical influences. Therefore, the formation of an amorphous film on the surface of a micromagnet is its natural protection from an aggressive external environment, when, for example, magnetic micropincers is used in the body *in vivo*. The laser engineering of the amorphous surface layer, the design of the amorphous „pattern" in specified areas, and the programmable creation of a domain structure in amorphous sections of microwires all open up new opportunities for improving micromagnets.

The objectives of the work are to select the parameters of laser processing, which leads to local amorphization of PrDyFeCoB crystalline microwires, as well as to detect and analyze the domain structure of the amorphized regions, and compare it with the domain structure of samples subjected to vacuum annealing.

2. Samples and experimental methods

Amorphous PrDyFeCoB microwires with a length of ~ 1 cm and a diameter of $\sim 50\,\mu$m were obtained by rapid cooling at a rate of about $\sim 10^6$ K/s by the suspended melt droplet extraction (SMDE) heated by a high-energy electron beam [5–8]. Figure 1, *a* shows a SEM image of the polished end of an amorphous microwire. For comparison,

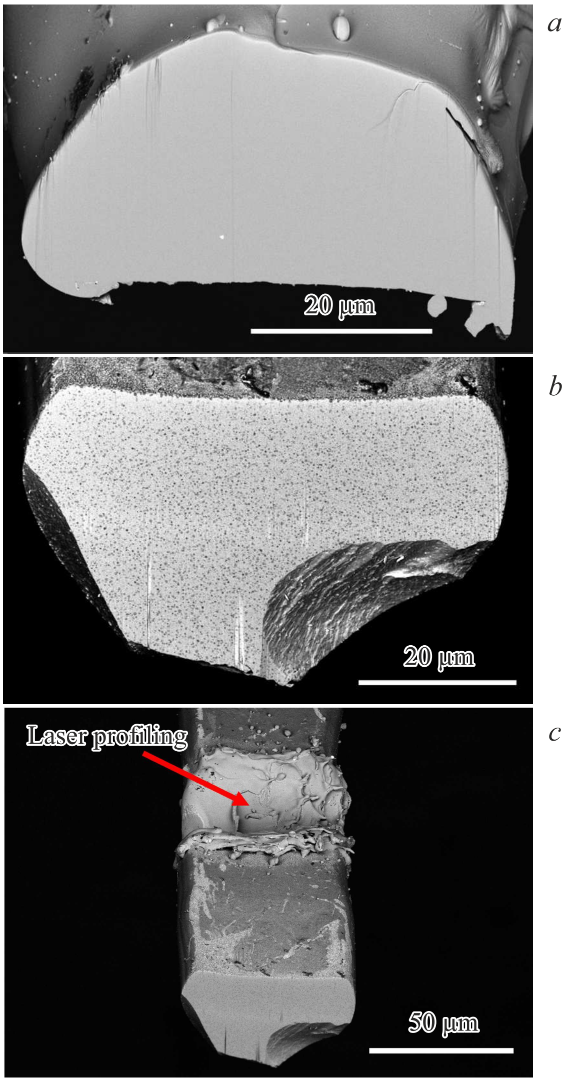

Figure 1. SEM-images of the polished end of an amorphous microwire: *a* — before annealing and *b* — after vacuum annealing, *c* — microwires after vacuum annealing and laser profiling.

Figure 1, *b* shows the cross-section in the same microwire after vacuum annealing at 900°C for 2 h at a pressure of 10^{-5} Torr.

The radiation from a pulsed ytterbium fiber laser G-MARK100 with a wavelength of 1070 nm focused by a lens F-100 (laser spot size 8–12 μm) was used for local laser profiling of the microwire after vacuum annealing. Profiling was carried out in air with a laser beam velocity of 850 mm/s, power of $P \approx 16$ W, pulse frequency of 25kHz, single pulse energy of 1 mJ and duration of 120 ns. Figure 1, *c* shows an example of a fragment of a microwire exposed to laser radiation.

The images of the microwires were obtained using a SUPRA 25 scanning electron microscope (SEM) (Zeiss). Electron diffraction was obtained using a high-resolution transmission electron microscope JEOL (HR TEM) at an accelerating voltage of 200 kV.

The integrated magnetic characteristics of the microwires were determined by SQUID magnetometry using MPMS XL Quantum Design magnetometer. Local magnetic hysteresis, visualization of magnetic domains, and the process of remagnetization of microwires were obtained using NEOARK Neomagnesia LiteBH-753 magneto-optical microscope, recording the Kerr effect (MOKE) in longitudinal geometry. The external magnetic field was directed along the axis of the microwire in all experiments.

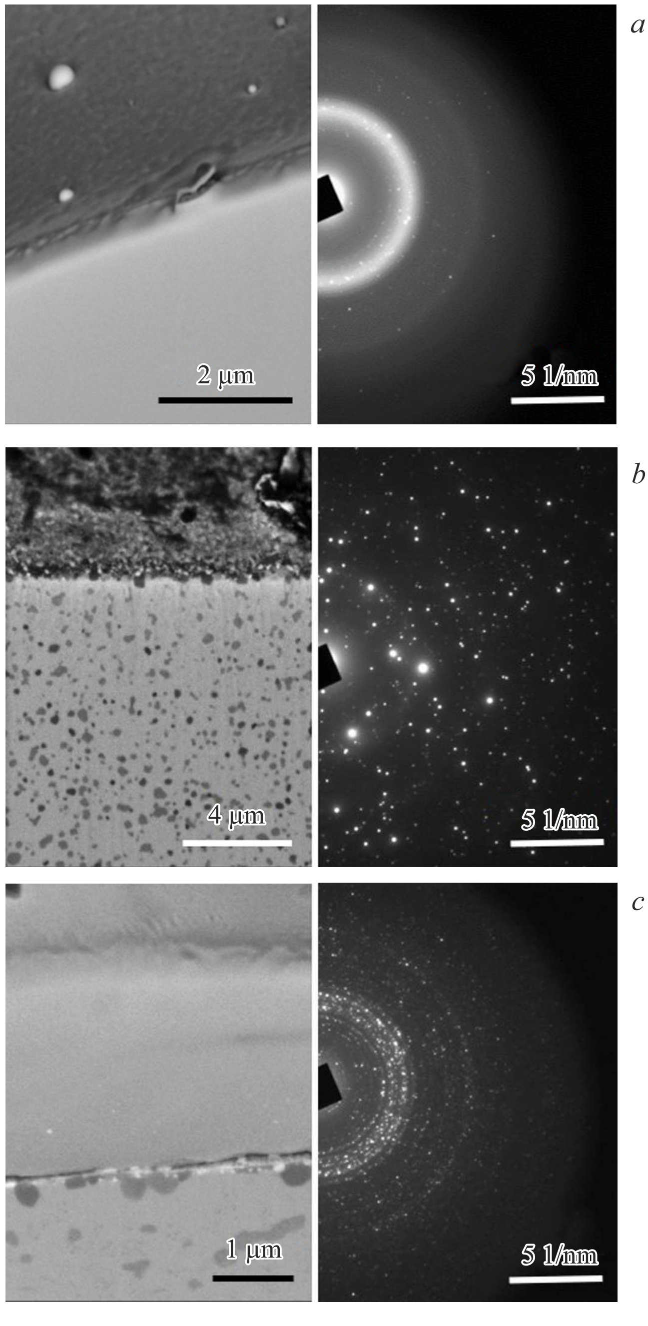

Figure 2. SEM images and corresponding electron diffraction patterns for lamellae: *a* — amorphous microwire, *b* — microwire after vacuum annealing, *c* — microwire after vacuum annealing and laser profiling.

3. Experimental results and discussion

The structure of the microwires looks homogeneous before annealing (Figures 1, *a* and 2, *a*) a chaotic but uniform distribution of dark inclusions is observed throughout the entire volume of the microwire after annealing (Figures 1, *b* and 2, *b*). The electron diffraction pattern of the macrowire before annealing has a characteristic halo with rare reflexes (Figure 2, *a*) corresponding to crystallites with the size of up to 10 nm. The crystallites most likely correspond to inclusions of 2-14-1-phase and appear in amorphous microwires when the cooling rate decreases from 55 to 50 m/s. Vacuum annealing results in the formation of a polycrystalline structure in amorphous microwires, as evidenced by a large number of point reflections and the absence of a halo on the electron diffraction pattern (Figure 2, *b*). Local laser profiling of a polycrystalline microwire causes local surface amorphization of the material up to a depth of 3 μm at the area of exposure to the laser beam, as evidenced by weak continuous halos on the SEM image in the vicinity of the molten section of the microwire. (Figure 2, *c*). The electron diffraction pattern of the lamella (Figure 2, *c*), cut from a section of a microwire subjected to laser irradiation, contains both point reflexes and weakly noticeable blurred rings, indicating the presence of crystallites in the amorphous material.

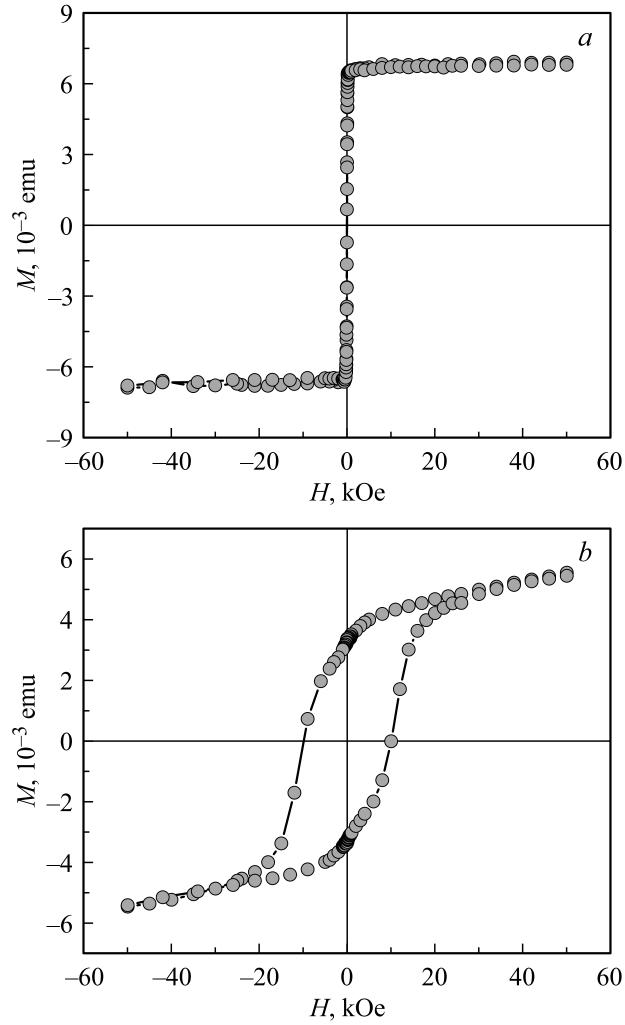

Figure 3. Magnetic moment hysteresis loops obtained using a SQUID magnetometer for the same microwire at a temperature of 300 K: *a* — before vacuum annealing and *b* — after vacuum annealing.

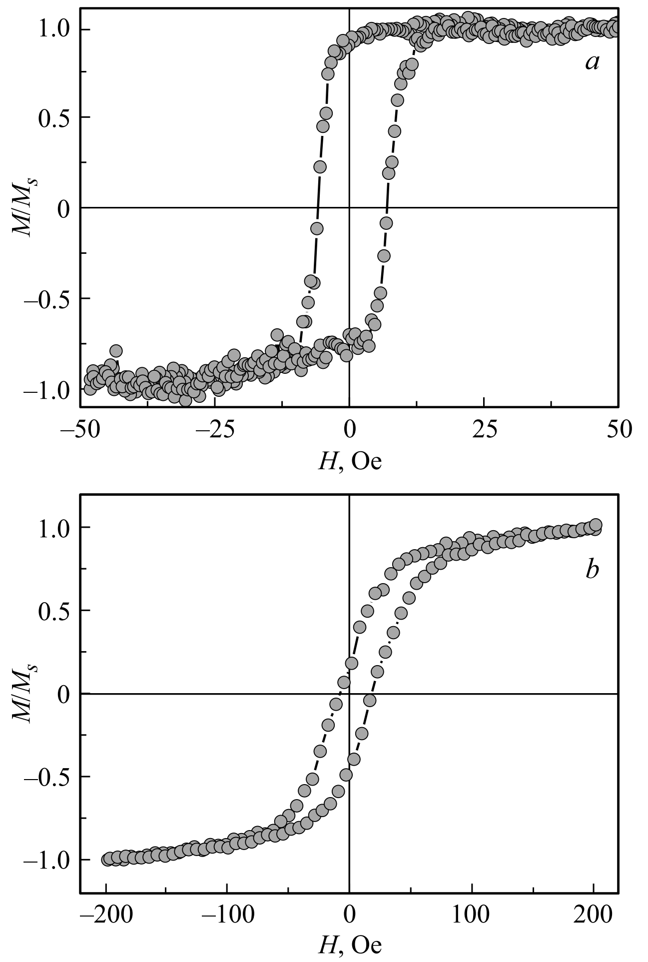

Figure 4. Magnetic hysteresis loops (M_S — saturation magnetization) obtained using a Kerr microscope at a temperature of 300 K on *a* — a section of the surface of an amorphous microwire before vacuum annealing and *b* — irradiated with a laser a section of an annealed microwire.

Figure 3 shows hysteresis loops obtained using a SQUID magnetometer for an amorphous microwire before annealing (Figure 3, *a*) and a polycrystalline microwire after vacuum annealing at 900°C (Figure 3, *b*). Amorphous microwires (Figure 3, *a*) are characterized by a narrow rectangular hysteresis loop with saturation in small fields of $\sim$ 150 Oe and a low coercive force of $\sim$ 8 Oe. Vacuum annealing causes a significant increase in the coercive force to $\sim$ 10 kOe (Figure 3, *b*) for polycrystalline microwires, while the magnetization does not reach saturation even in the fields of $\sim$ 50 kOe, which is attributable to the formation

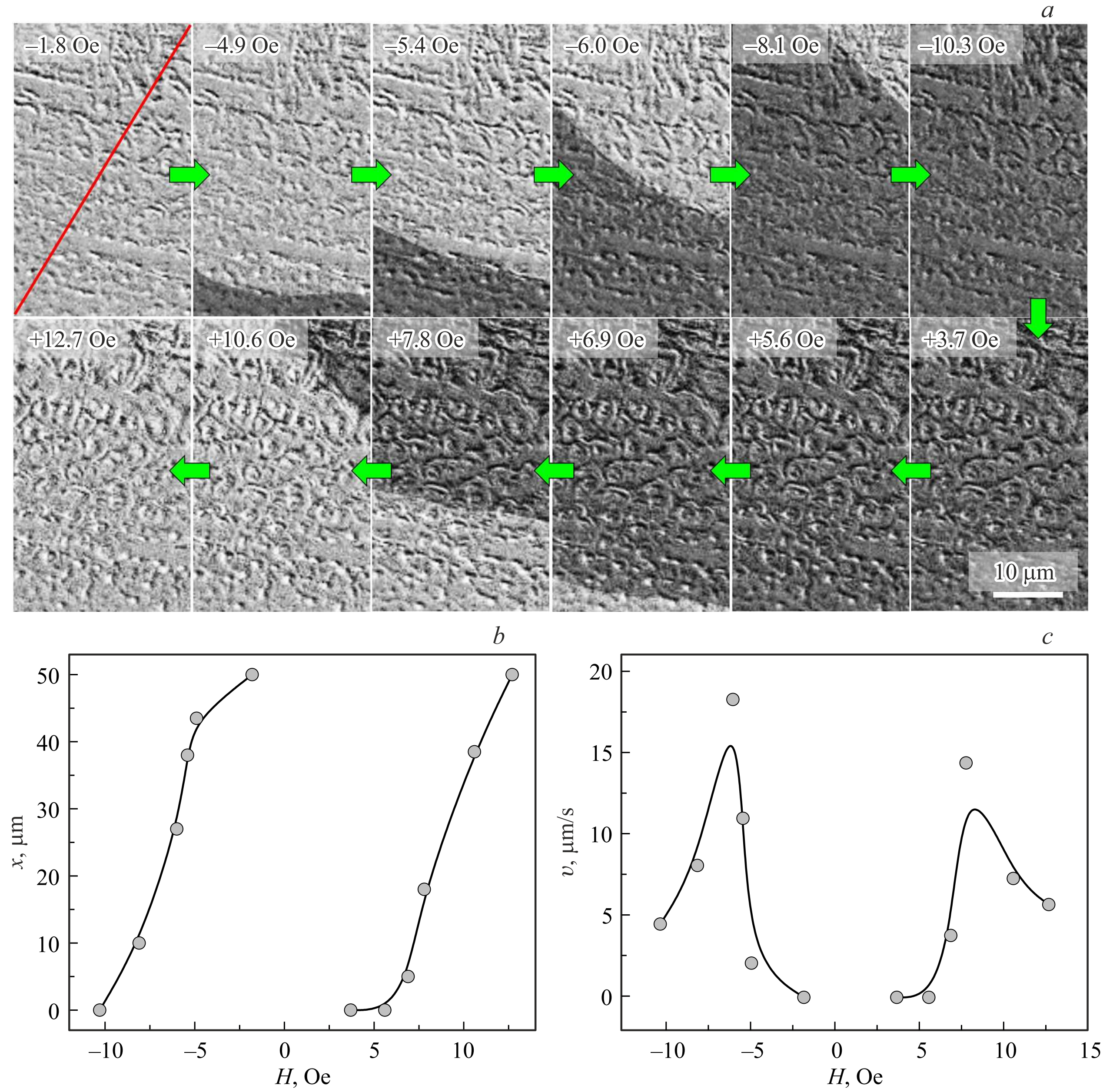

Figure 5. A sequential change of the domain structure of the amorphous microwire section (a) and the dependence of the coordinate (b) and velocity (c) of the domain wall on the field for the direction along the diagonal of the figure (shown by the red line). The field scan rate is 1 Oe/s. x — the coordinate of the domain wall along the red line on the panel (a).

of a rigid magnetic phase of the 2-14-1 type. The presence of steps on the hysteresis loop in small fields (Figure 1, b) indicates the presence of two phases simultaneously in polycrystalline microwires: hard magnetic, highly coercive phase 2-14-1 and the soft magnetic phases 1-4-1 and 2-1.

Figure 4 shows local loops of magnetic hysteresis obtained using a Kerr microscope for a section on the surface of an amorphous microwire (Figure 4, a) and a section of a polycrystalline microwire subjected to laser profiling (Figure 4, b). It was not possible to record a local magnetic hysteresis loop using the Kerr method for a microwire after thermal annealing, since the maximum field value of $\sim$ 1,kOe was insufficient to remagnetize the sample. Magnetization hysteresis M with coercive force of $\sim$ 10 Oe and saturation in small fields of $\sim$ 20 Oe is observed in the initial amorphous microwire (Figure 4, a). The value of the coercive force in the laser-amorphized section of the microwire is $\sim$ 10 Oe like in the amorphous microwire, while the loop acquires an oblique shape with a saturation field of 200 Oe. This fact indicates the proximity of the structural states of the initial amorphous material and material which is amorphized under the action of a laser.

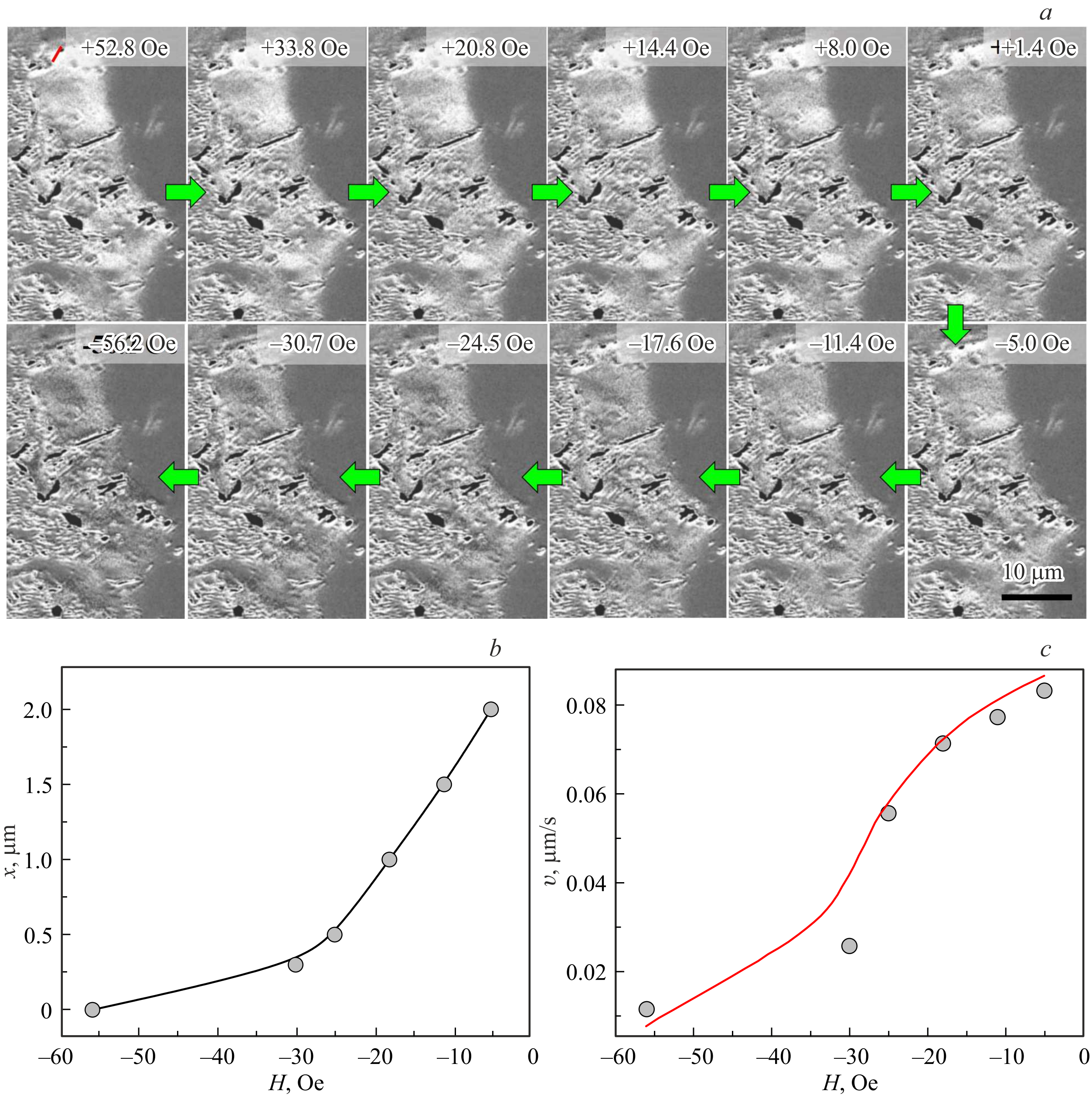

Figure 6. A sequential change of the domain structure of the section of the microwire (a) subjected to vacuum annealing and subsequent laser irradiation, and the dependence of the coordinate (b) and the velocity of the domain wall (c) on the field for the direction along the red line. The solid line shows the approximation of the dependence $\nu(H)$ by the formula (1). The field scan rate is 1 Oe/s. x — domain width in the area along the red line on the panel (a).

Figures 5 and 6 show images of the domain structure of an amorphous microwire (Figure 5, a) and a section of a polycrystalline microwire after laser irradiation (Figure 6, a). It was not possible to register the domain structure using a Kerr microscope for a polycrystalline microwire without laser profiling. The domain boundary and its movement (movement of light and dark contrasts) are visible in the amorphous microwire (Figure 5, a), remagnetization occurs by domain expansion with a change in the magnitude and direction of the external magnetic field. It should be noted that, although we observe a longitudinal component of magnetization in this paper, we established earlier using the method of magneto-optical indicator films (MOIF) [8] the presence of domains with radial magnetization in the surface layers [9] in the same PrDyFeCoB microwires. This indicates that the total magnetization of the microwire is directed at an angle to its axis. Figures 5, b and 6, b show the dependences of the domain wall coordinate and its velocity on the external magnetic field. This is also evidenced by the rather high velocity of the domain wall of $\sim 18\,\mu$m/s (Figure 5, b). The non-monotonic dependence of the velocity of the domain wall on the magnetic field is typical for the transition regime from the domain wall creep in a weak field to its sliding in fields of above 8 Oe [10].

Vacuum annealing of amorphous microwires leads to the disappearance of the domain structure in a weak field of up to 1 kOe. However, local laser irradiation of polycrystalline annealed microwires restores the domain structure in them (Figure 6, *a*). The size of the domains decreases in this case, and their arrangement becomes chaotic compared to the domains in the original amorphous sample (Figure 5, *a*). The dynamics of domains in laser-irradiated samples also differs from the dynamics of domains in the initial amorphous samples (Figure 5, *a* and *b*). The velocity of the domain wall movement in the locally irradiated regions is two orders of magnitude lower than in the initial completely amorphous microwire of $\sim 0.1\,\mu$m/s. Therefore, the dependence of the velocity on the magnetic field is monotonous, and the transition phase of the dependence $\nu(H)$ to the sliding mode of the domain wall is not observed (Figure 6, *c*).

The dependence of the velocity of the domain wall on the magnetic field in the creep mode is described by the formula [11]:

$$\nu(H) = \nu_0 \exp\left(-\frac{U}{k_B T}\left(\frac{H_c}{H}\right)^{1/4}\right), \qquad (1)$$

where U — height of the potential barrier, k_B — Boltzmann constant, T — temperature, H_c — critical field. The critical field established using the approximation of Figure 6, *c* is $H_c = -55$ Oe in our experiments.

Thus, the dynamics of domain walls in fully amorphous and partially amorphous laser microwires differ in terms of velocity and modes of movement of the domain wall in them.

Conclusions

1. The annealing of an amorphous DyPrFeCoB microwire results in the formation of a polycrystalline hard magnetic phase 2-14-1 and in a significant increase of the coercive force from 8 Oe for amorphous microwires to 10 kOe for polycrystalline microwires.

2. The local laser profiling in polycrystalline DyPrFeCoB microwires prepared by vacuum annealing leads to the occurrence of an amorphous surface layer with a thickness of $\sim 3\,\mu$m and to a narrowing of the hysteresis loop compared with the initial polycrystalline microwire.

3. Domains are observed in the amorphous part of the microwire and they completely disappear under the action of vacuum annealing. Local laser irradiation results in the occurrence of small and randomly located domains in the area of the laser tag.

4. The dependence of the velocity of the domain wall on the field is consistent with the creep regime in the irradiated regions, in which the domain wall thermally overcomes obstacles such as inhomogeneities of the amorphous phase. The dependence of the velocity of the domain wall on the field is nonmonotonic in a fully amorphous microwire not subjected to laser irradiation and annealing, and the velocity of movement is two orders of magnitude higher than in local amorphous regions. This indicates the transition of the creep mode to the sliding mode in completely amorphous microwires, as well as different drag mechanisms in fully and partially amorphous microwires.

Funding

The study was carried out within the framework of the state assignment of the Federal Research Center for Problems of Chemical Physics and Medical Chemistry of the Russian Academy of Sciences 124013100858-3.

Conflict of interest

The authors declare that they have no conflict of interest.

References

[1] C.-H. Lambert, S. Mangin, B.S.D.C.S. Varaprasad, Y.K. Takahashi, M. Hehn, M. Cinchetti, G. Malinowski, K. Hono, Y. Fainman, M. Aeschlimann, E.E. Fullerton. Sci. **345**, *6202*, 1337 (2014).
[2] J. Igarashi, Q. Remy, S. Iihama, G. Malinowski, M. Hehn, J. Gorchon, J. Hohlfeld, S. Fukami, H. Ohno, S. Mangin. Nano Lett. **20**, *12*, 8654 (2020).
[3] O. Koplak, K. Kravchuk, A. Useinov, A. Talantsev, M. Hehn, P. Vallobra, S. Mangin, R. Morgunov. Appl. Surf. Sci. **493**, 470 (2019).
[4] S. Iihama, Y. Xu, M. Deb, G. Malinowski, M. Hehn, J. Gorchon, E.E. Fullerton, S. Mangin. Adv. Mater. **30**, *51*, 1804004 (2018).
[5] O.V. Koplak, E.V. Dvoretskaya, D.V. Korolev, R.A. Valeev, V.P. Piskorskii, M.V. Gapanovich, Yu.S. Pogorelets, R.B. Morgunov. Phys. Solid State **63**, *11*, 1675 (2021).
[6] O.V. Koplak, E.V. Dvoretskaya, D.V. Korolev, R.A. Valeev, V.P. Piskorskii, A.S. Denisova, R.B. Morgunov. Phys. Solid State **62**, *8*, 1333 (2020).
[7] O.V. Koplak, E.V. Dvoretskaya, V.L. Sidorov, N.N. Dremova, I.V. Shashkov, D.V. Korolev, R.A. Valeev, V.P. Piskorski, R.B. Morgunov. J. Surf. Invest.: X-Ray, Synchrotron Neutron Tech. **15**, *2*, 292 (2021).
[8] O.V. Koplak, V.L. Sidorov, E.V. Dvoretskaya, I.V. Shashkov, R.A. Valeev, D.V. Korolev, R.B. Morgunov. Phys. Solid State **63**, *2*, 266 (2021).
[9] V.I. Nikitenko, V.S. Gornakov, L.M. Dedukh, A.F. Khapikov, L.H. Bennett, R.D. McMichael, L.J. Swartzendruber, A.J. Shapiro, M.J. Donahue, V.N. Matveev, V.I. Levashov. J. Appl. Phys. **79**, *8*, 6073 (1996).
[10] V.S. Gornakov, L.M. Dedukh, V.I. Nikitenko, V.T. Synogach. JETP **63**, *6*, 1225 (1986).
[11] S. DuttaGupta, S. Fukami, C. Zhang, H. Sato, M. Yamanouchi, F. Matsukura, H. Ohno. Nature Phys. **12**, *4*, 333 (2016).

Translated by A.Akhtyamov